A unified phenomenological analysis of the experimental velocity curves in molecular motors

Aleix Ciudad[a] and J. M. Sancho
Department d'Estructura i Constituents de la Matèria, Facultat de Física, Universitat de Barcelona, Diagonal 647, E-08028 Barcelona, Spain

(Received 21 November 2007; accepted 6 May 2008; published online 12 June 2008)

We present a unified phenomenological kinetic framework to analyze the experimental data of several motor proteins (either linear or rotatory). This formalism allows us to discriminate the characteristic times of most relevant subprocesses. Explicitly, internal mechanical as well as chemical times are taken into account and joined together in a full-cycle time where effusion, diffusion and chemical rates, viscoelastic friction, and overdamped motion are considered. This approach clarifies the most relevant mechanisms in a particular motor by using the available experimental data of velocity versus external load and substrate concentration. We apply our analysis to three real molecular motors for which enough experimental data are available: the bacterial flagellar motor [Yoshiyuki *et al.*, J. Mol. Biol. **377**, 1043 (2003)], conventional kinesin (kinesin-1) [Block *et al.*, Proc. Natl. Acad. Sci. U.S.A. **100**, 2351 (2003)], and a RAN polymerase [Abbondanzieril, Nature (London) **438**, 460 (2003)]. Moreover, the mechanism of stalling a motor is revised and split into two different concepts (mechanical and chemical stalling) that shed light to the understanding of backstepping in kinesin-1. © *2008 American Institute of Physics*.
[DOI: 10.1063/1.2937452]

I. INTRODUCTION

Several molecular functions such as directional transport of chemical substances, active motion, cell division, genetic transcription, etc., are performed by molecular engines. These machines operate as mechanical nanomotors transforming chemical (i.e., nucleotide hydrolysis) or electrochemical potential (ion flux) into mechanical work. Mechanical observables are now experimentally accessible being the mean velocity, linear or angular, the better studied quantity.[1–3,5–8] The behavior of this velocity is evaluated as a function of different and well controlled variables, such as the external load or the concentration of the specific substrate. The obtained velocity curves are very useful to analyze biochemical and mechanical properties and are a major criterion for evaluating different theoretical modellings. Several approaches have been proposed such as Kramers rates,[8] masters equations for chemical steps,[9] ratchetlike Langevin equations,[10] etc., Kramers-type rates are based in the kinetics to overcome energetic barriers.[8,9,11] The reaction coordinate is identified with the direction of motion or with a projection on this direction, in such a way that when an external force is applied, the barrier increases with the force. In the master equation approach a set of transition probabilities for a set of assumed different chemical steps are proposed. Within this chemical scenario, mechanical variables such forces and spatial steps are difficult to incorporate and some important assumptions have to be made.[9,12] On the other hand ratchetlike models are more mechanical but chemical ingredients, such as ATP (Adenosine triphosphate) hydrolysis, are not so simple to incorporate in the modelings. Nevertheless, it is clear that molecular motors involve chemical and mechanical aspects that cannot be separated and have to be worked together in any modeling.

However, the above mentioned modeling is not the only possible way to study such type of devices. We know that a molecular motor operates in a succession of cycles where each cycle is composed of different subprocesses. Not all of them are necessarily mediated by energetic barriers. There can be entropic barriers[13] or other type of processes that are not directly coupled to displacement of the center of mass of the motor.

In this work we will focus on the different subprocesses that can be relevant in this problem, determining which are dominant and which are less relevant. Our approach has enough generality to be applied to three very different devices: a rotatory motor such as the bacterial flagellar motor (BFM);[1] and two linear motors: a conventional kinesin (kinesin-1)[2] and a RNA polymerase (RNAp).[3]

Specifically we postulate that the most relevant quantity is the characteristic time of each subprocess, from which the contribution to the mean velocity can always been obtained. Let t_j be the time (often stochastic) of a subprocess in the motor cycle with a fixed L or $\Delta\theta$ (linear or angular) step displacements per cycle, respectively. Then, if this cycle is composed of the subprocesses $1,2\cdots n$, acting in succession, the average total time $\langle t\rangle$ of the cycle can be expressed as

$$\langle t\rangle = \langle t_1\rangle + \langle t_2\rangle + \cdots + \langle t_n\rangle, \tag{1}$$

and the mean velocity $\langle v\rangle$ or the angular velocity $\langle\omega\rangle$ are,

$$\langle v\rangle = \frac{L}{\langle t\rangle}, \quad \langle\omega\rangle = \frac{\Delta\theta}{\langle t\rangle}. \tag{2}$$

[a]Electronic mail: aleixciudad@gmail.com.

The latter expression can derived from the definition of mean velocity (total displacement divided by total time) for a trajectory that has undergone n cycles,

$$\langle v\rangle = \frac{\Sigma_{i=1}^{n}\Delta x_i}{\Sigma_{i=1}^{n}\Delta t_i} = \frac{nL}{\Sigma_{i=1}^{n}\Delta t_i} = \frac{L}{\langle t\rangle}, \tag{3}$$

where $\Delta x_i = L$ is the displacement performed in each cycle i and Δt_i is the time elapsed in the cycle. The formula is strictly valid only for motors that perform all the cycles with the same step size. However, it can be generalized for the case of a protein performing steps of different sizes mL (where $m=1,2,\ldots$) provided that we know the relative frequencies in which each step size appears. Such an expansion could be applied for the variable step size of Myosin V.[14]

Note that these expressions are strictly valid only when the transitions between the subprocesses are irreversible. However, in a protein motor it is reasonable to suppose such an irreversibility, since the chemical-potential differences are considerably bigger than the thermal energy. Even if some backward transitions can be observed experimentally, the do not affect substantially to the mean velocity value.

From now on we will work with time averages, even though we do not write them explicitly. Since we will assume that both L and $\Delta\theta$ are fixed or known from experimental data, we only have to concern about the subprocess times. The study of fluctuations is a second order improvement not considered in this work in an explicit way (although the effect of temperature is considered in the process of diffusion). This does not mean that higher momenta in the velocity distribution are not important, but a global understanding of the mean value is already lacking, so we will focus on this leaving a more refined description for further work.

We will consider three dominant types of subprocesses, although certainly there are more that may correspond to a second order or more refined description. First, we suppose that there is always a time scale for the motor to perform internal tasks that do not depend either on the external force f_{ext} or the substrate concentration $[S]$. An example of this could be the rate of ADP (Adenosine diphosphate) release in kinesin-1 after ATP binding in the attached head. We call this the *internal time* t_i. On the one hand, the motor needs some time to displace or to rotate in the fluid media. We call it the *mechanical time* t_m which can be evaluated using overdamped dynamics and that will be load dependent. On the other hand the energetic substrate, i.e., the nucleotides or the ions, employ some time to diffuse and bind the motor. Here diffusion and diffusion play an important role, and classical chemical kinetic theory provides theoretical tools to evaluate it. We call this the *chemical time* t_{chem}, which will be both load and energy substrate dependent. All these three characteristic times operate successively in every cycle and are of different natures.

Before ending this introduction some comments are in order. Two types of forcing are used in the experiments: conservative and nonconservative. From the three motors that we will analyze in this work, two of them use a conservative force (kinesin and RNAp) and one uses a nonconservative force (BFM). When utilizing optical tweezers (kinesin, RNAp), the applied force is directly a momentum transfer to the bead and, by extension, to the motor. Thus one can obtain the work performed by the motor by simply multiplying the value of the force by the total displacement. In the nonconservative case, the forcing is introduced through different bead sizes and its corresponding nonconservative Stokes friction forces. The substrate that attach molecular motors is quite different from motor to motor. In BFM is a flux of ions forced by an electrochemical potential, while in kinesin of RNAp are NTP-like nucleotides. NTP is the general notation for {ATP,UTP,GTP,CTP}, where the last three nucleotides are Uridine triphosphate, Guanosine triphosphate and Cytidine triphosphate, respectively.

This paper is organized as follows. In the next section we present the theoretical approach. Section III is devoted to the application of our predictions to three different molecular motors and the comparison of our results to experimental data. Finally, we end with some conclusions.

II. THEORETICAL APPROACH

In this section we present a detailed analysis of the three main time scales already introduced. Each characteristic time will be treated separately in order to address its specific processes involved.

A. Mechanical and internal times

Molecular motors move in a viscous media where inertia is suppressed by the friction. As a result, the dynamics are governed by the second Newton's law without the acceleration term. To lowest order, thermal fluctuations are not required to obtain explicit predictions for the motor mean velocity. For an overdamped motor which is able to exert a constant motive force f_m along a single direction, the mean velocity can be written as

$$\langle v\rangle = \frac{1}{\gamma_t}(f_m + f_{\text{ext}}), \tag{4}$$

where f_{ext} is the external load and γ_t the translational drag coefficient. A negative value of f_{ext} signifies useful work from from the motor. From Eq. (4) we can get the expression of the mechanical time,

$$t_m = \frac{\gamma_t L}{f_m + f_{\text{ext}}}, \tag{5}$$

where the mechanical stall force is found at $f_m + f_{\text{ext}} = 0$.

In the case of a rotatory motor (with no conservative forces), we have instead

$$(\gamma_r + \gamma_{\text{ext}})\omega = \tau_m, \tag{6}$$

where γ_r is the rotational drag coefficient of the motor, γ_{ext} if the friction of the bead attached to the motor, and τ_m the motive torque. The mechanical time is obtained as in Eq. (5).

From Eqs. (4) and (6) one can define the maximum physical velocities in the absence of a load,

$$\langle v\rangle_m = \frac{1}{\gamma_t}f_m, \quad \langle\omega\rangle_m = \frac{1}{\gamma_r}\tau_m. \tag{7}$$

It is worth mentioning that the above analysis is obviously incomplete and we need to consider additional types of subprocesses in the cycle. Indeed, the mechanical time alone cannot be responsible for the mean velocity values observed experimentally for linear motors, while for rotatory motors it is better to use a more sophisticated expression such as in Ref. 1. Let us start with a simple analysis of this problem. First we take that the viscosity of the water is $\eta=10^{-9}$ pN s/nm^2, and the translational drag coefficient is $\gamma_t=6\pi\eta R$, where R is the radius of the molecule. Using these data we can estimate approximately the maximum velocity expected in kinesin-1 or in RNAp. Silica beads in these cases have typically $R\sim 0.5$ μm. In kinesin experiments, typical motive forces are of the order of 5 pN. As a result, we expect $\langle v\rangle_{\max}\sim 500$ μ/s, which is a value more than 500 times the experimentally measured maximum velocity. For the RNAp, typical forces are approximately 25 pN. We can then made an estimate of $\langle v\rangle_{\max}\sim 2500$ μ/s, a value that is about
5×10^5 times the experimental velocity. From the above calculations it follows that other times scales are involved in the cycle.

The next simple correction to the mechanical time is to assume the existence of an internal time. In fact, every motor needs a time to perform internal jobs that are not necessarily force or substrate dependent and during which internal process are performed.

For example, in kinesin-1 the rate of phosphate release in the microtubule-attached head or the rate for ADP release in the other head may be candidates for such type of processes. In BFM, the time for the ion to cross the membrane does not necessarily depend on the potential difference between both sides. In general, if there were no such processes, at zero load (or at high assisting forces) and at very high substrate concentrations, the mean velocity would not saturate to a finite value. In this saturating regime, the maximum velocity is approximately proportional to the inverse of these internal times. Then, we denote this time by t_i and we assume it takes a constant value specific of each motor. As a result, the total mean time $\langle t\rangle$ for a cycle is $\langle t\rangle=t_i+t_m$, while the mean velocity (2) becomes

$$\langle v\rangle=\frac{L}{t_i+\dfrac{\gamma_t L}{f_m+f_{\text{ext}}}}. \tag{8}$$

In Fig. 1 we plot force-velocity curves where the influence of the internal time is manifested in reducing the final velocity.

B. Chemical time: The pocket model approach

Checking the experimental data of any molecular motor it becomes clear that both mechanical and internal times are not enough. We have to consider that there is a certain time used to wait for the substrate which is diffusing in the media. Experimentally, it has been found that the chemical times follow Poisson distribution with, for example, a mean time of about 50 ms in the case of highly loaded kinesin. [6,15] If the

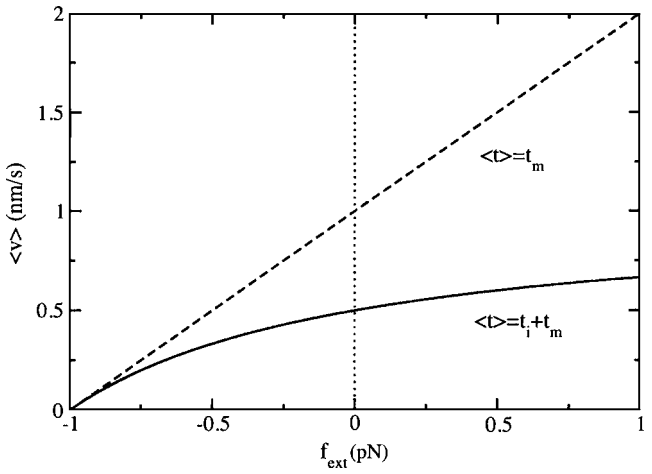

FIG. 1. Mean velocity $\langle v\rangle$ vs an external force f_{ext}. Dashed line for a process with only mechanical time. Continuous line for a process with mechanical and internal time. For the sake of simplicity, we have chosen $L=1$ nm, $\gamma_t=1$ pN s/nm, $f_m=1$ pN, and $t_i=1$ s.

substrate concentration is low, these times will increase, while for a very high concentration are reduced, but never this time scale goes to zero.

After substrate binding, some chemical subprocesses take place. The kinetics of these steps is described by the so-called Michaelis–Menten equation, which states that the velocity of reaction involves two different time scales where the substrate binding follows the mass action law.

Moreover it has been observed that this chemical time increases with an opposing load. [5] This is quite a surprising fact. If the load is applied to the motor without affecting the substrate conditions, why does the substrate take longer to reach the motor when the load is applied? Some explanations have been proposed. [9,12] The common scenario is to explicitly give the chemical potential along the reaction coordinate and to map this coordinate into the spatial position in such a way that the reaction takes place when an energetic barrier is surmounted. The problem with this approach is that the load affects the chemical potential in a way that it vanishes at stalling conditions. This means that the reactants and the products are at equilibrium. Such a consequence may hold for reversible motors such as BFM, but we will see that for these devices the load dependence of the chemical time is not relevant. In mechanoenzymes as kinesin-1 or RNAp, however, the load dependence of t_{chem} is crucial. Even at stalling loads the chemical equilibrium is hardly affected between the reactants and products. In fact, the approximation that the reaction takes place irreversibly still holds well. If we would follow an energetic wall model modulated by Boltzmann factors, we would arrive to the conclusion that the kinesin motor at stalling conditions would be able to synthesize an ATP, for instance. This is not what happens in reality, since kinesin still hydrolyzes even at backstepping. Then, we cannot introduce the load in the chemical potential because such a potential may be kept approximately constant at all regimes of the load. Instead, we propose to introduce the external force through a simple effusion model. Following the law of mass action, we suppose that there is a time for the substrate to enter into the cavity that is inversely

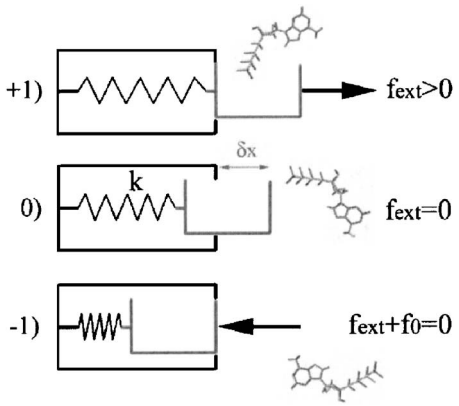

FIG. 2. Scheme for a simple linear pocket model, given by a box with an opening door that depends on the external load. In (0) we have the pocket without load, and it has a certain natural opening. In (+1) we can see the extreme case for an assisting load, where the pocket is totally opened and the substrate, represented here by an ATP molecule, can easily bind the cavity. Finally, in (−1) we can see the effect of a large opposing force. For $f_{\text{ext}}=-f_0$ the cavity becomes completely closed.

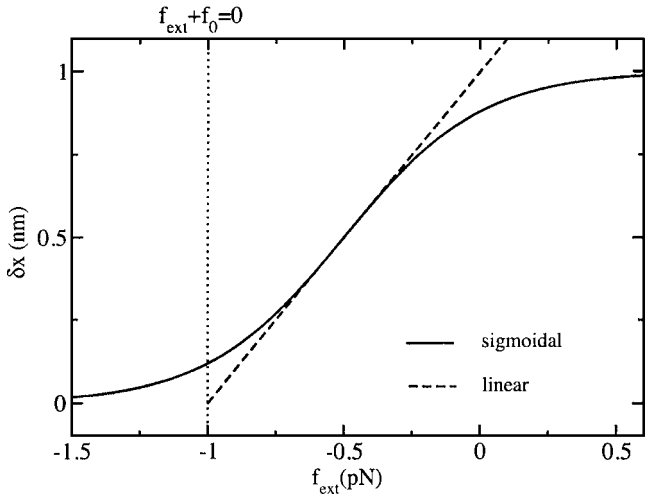

FIG. 3. Opening of the pocket as a function of the external load. The solid line corresponds to the sigmoidal version, while the dashed corresponds to the linear case. All the parameters are set equal to unity.

proportional to the substrate concentration. Furthermore, classical kinetic theory states that the effusion time for a particle to cross a hole of a certain area is proportional to the inverse of this area. By hypothesis, we suppose that this area is affected by the load in such a way that it decreases at opposing loads and it increases at assisting loads. In such a model, the enzymatic activity is not supposed to be changed by the load. For kinesin-1 and RNAp it is a reasonable supposition, while for the F_O part of the ATP synthases we should also take into account the effect of the load on the catalytic processes. In other words, we propose a model where the binding of the substrate is not mapped into the position of the motor but it relies on an internal conformation of the protein. Moreover, the enzymatic activity is neither mapped into the position, i.e., the progress along the chemical potential is not associated with a displacement of the center of mass of the motor. Only the mechanical motion is linked with the position of the motor, which allows to separate mechanical stepping (which can be forward or backward) and chemical hydrolysis (which in our model is supposed to be forward all the time). Such a separation is necessary since the experiments in Ref. 6, as the mechanical cycle can be inverted while the chemical cycle keeps going forward.

Thus, let us consider that the binding site is a cavity where the substrate has to enter (Fig. 2), as it was claimed in Ref. 16. Then, under the influence of an opposing load, the cavity may be strained and thus less accessible to the substrate. As we have already mentioned, the binding process can be interpreted as an effusion process where the load controls the area of the hole to enter the substrate. Then, a different stall force (here called chemical or entropic) can be defined as the force that completely closes the pocket and accordingly the chemical time becomes infinite. This concept of chemical stalling is different from the mechanical stall force, where the opposing load equilibrates the motive force of the motor. Our analysis thus predicts that the motor can be stalled by two different mechanisms.

To implement analytically this idea we propose the simple mechanism shown in Fig. 2. In order to give an expression for the rate of the substrate entering into the pocket, we shall consider a pocket which has a hole of area $a\delta x$, where a is the width and $\delta x=\delta x(f_{\text{ext}})$ is the load dependent aperture of the hole. Then the effusion time for a small diffusing particle to enter into the hole is inversely proportional to the substrate concentration and to the opening area of the cavity, i.e., $\propto 1/a[S]\delta x$. Note also that the size of the substrate is comparable to the opening of the pocket, so there is a certain orientation for the molecule to match the cavity (as illustrated in Fig. 2). This is the effect of final adhesion to the pocket, which is supposed at first approximation to be dependent on the accessible surface but independent of the substrate concentration. Consequently we have to include this last effect as a constant contribution $\sim 1/\delta x$. Adding these two time scales and grouping the free parameters, the chemical time is

$$t_{\text{chem}} = \frac{1}{\delta x}\left(A + \frac{B}{[S]}\right), \tag{9}$$

where A and B are two constants to determine. This is not more than a quite general expression for the mass action law. Notice that the independent term, proportional to A, is substrate shape dependent but $[S]$-independent. To illustrate this idea, we can consider the case of Uracile base in RNAp. For a given pocket, four different substrates can bind in it, and all of them have different binding rates. Despite their molar mass and Graham's law effects, the Uracile nucleotide UTP has a very low rate considering that it is a relatively light nucleotide. It has an addition rate about three times slower than CTP, which is very similar in molecular weight. Surely this is due to orientation and steric contributions near the pocket. It is interesting that the explicit form of Eq. (9) can be mapped into mixed inhibition scheme in enzymatic theory.

The point now is to guess how this time has to depend on the external force. We can assume, following Fig. 3, that

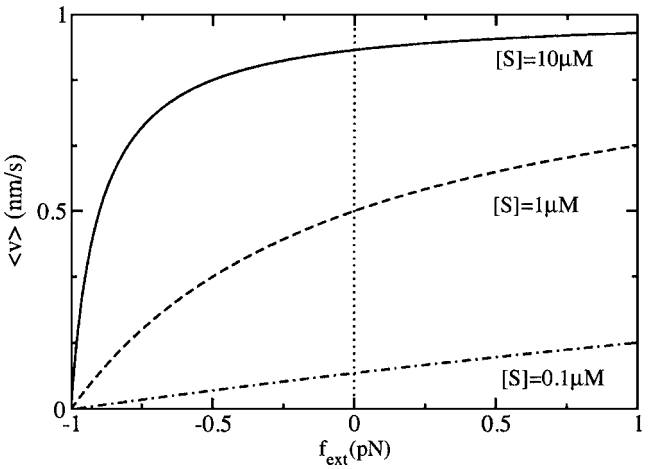

FIG. 4. Mean velocity vs external force when we have an internal time plus a chemical time, i.e., $\langle t\rangle = t_i + C/[S](f_{\text{ext}}+f_0)$. We set $t_i=1$ s, $f_0=1$ pN, and $C=1$ s pN μM. Continuous, dashed, and dash-dotted lines correspond to $[S]=10$, 1, and 0.1 μM, respectively.

the pocket has an elastic opening that is stressed when the load is applied. Assuming a linear spring we can propose the dependence

$$\delta x = \frac{f_0 + f_{\text{ext}}}{k}, \tag{10}$$

where k is the effective stiffness and f_0 corresponds to the chemical stall force: when $f_{\text{ext}}=-f_0$ the hole is closed. For $f_{\text{ext}}=0$ we have the natural opening, and for $f_{\text{ext}}>0$ the hole has more accessible surface.

In Fig. 4 we show plots of the mean velocity when internal and chemical times are joined. We show force-velocity curves for three different substrate concentrations. One can note that the curvature of the plots strongly depends on the concentration. The reason for the plateau in the high concentration case is that the substrate binding is not rate limiting, as it was experimentally observed.[2,5]

Although the linear spring pocket model is very useful to illustrate the idea of the pocket kinetics, it is convenient to introduce a more sophisticated version of the model in order to have more accurate predictions. However, the philosophy remains exactly the same. Instead of a linear spring response it is more realistic to consider a nonlinear response of the pocket that is still linear at low forces and bound at extreme loads. This is achieved by using a sigmoidal function,

$$\delta x = \frac{l_x}{2}\left[1 + \tanh\left(\frac{2}{kl_x}(f_0 + f_{\text{ext}}) - 1\right)\right], \tag{11}$$

where l_x is the longitudinal size of the pocket. We can see how we recover the linear case for $\tanh x \sim x$. Then, we still can talk about a stiffness of the pocket. The price is the introduction of a new parameter l_x.

In Fig. 3 we plot the dependence of δx under an external load. The main difference between the linear and the sigmoidal cases is that in the latter case the pocket never closes completely.

C. The generic formula

Once we have all the times involved in a single cycle, we can write down the whole expressions (1) and (2) for the velocity of a linear motor as a function of $[S]$ and f_{ext},

$$\langle v\rangle = \frac{L}{t_i + \dfrac{\gamma_i L}{f_m + f_{\text{ext}}} + \dfrac{1}{\delta x}\left(A + \dfrac{B}{[S]}\right)}, \tag{12}$$

with δx given by expressions either (10) or (11). For the rotatory motor we can write the equivalent expression as

$$\langle \omega\rangle = \frac{\Delta\theta}{t_i + \dfrac{\Delta\theta(\gamma_r + \gamma_{\text{ext}})}{\tau_m} + \dfrac{1}{\delta x}\left(A + \dfrac{B}{[S]}\right)}, \tag{13}$$

where δx will be considered a constant for the case of BFM analyzed in this work. These last two equations are the main result in this paper. We will start now analyzing the consequences, properties, and utility of these formulas.

As we have predicted before, there are two possible values of the external force that can stall the motor, i.e., f_0 and f_m. When f_{ext} equals one of these values with opposite sign, then the motor stalls either chemically or mechanically, respectively. If $f_{\text{ext}}+f_0=0$, then $t_{\text{chem}}\to\infty$ and the velocity vanishes because no substrate can bind the pocket. If $f_{\text{ext}}+f_m=0$, $t_m\to\infty$, and then the motive force cannot drive the motor anymore. This scenario is interesting since the experimental definition of stall force f_S is unique, that is, the force at which the motor stops.

Let us analyze the three possible cases. If $f_m=f_0$, both stall forces are the same. When, $f_m>f_0$, the first limiting factor would be chemical. This means that even if the motor could exert more force, no substrate can bind the pocket and no motion is produced. The last case occurs when $f_m<f_0$. This is the most interesting because when the motor is mechanically stalled, it still can bind substrate. Moreover, if we apply now a load such that $f_{\text{ext}}+f_m<0$ but $f_{\text{ext}}+f_0>0$, then the motor will tend to move backward but still consuming the energy of the substrate. To characterize analytically this backstepping we write expression (12) as

$$\langle v\rangle = \frac{L}{t_i + \dfrac{\gamma_t L}{f_m + f_{\text{ext}}} + \dfrac{A}{\delta x} + \dfrac{B}{\delta x[S]}}\ \text{sign}[f_m + f_{\text{ext}}], \tag{14}$$

$$f_0 + f_{\text{ext}} > 0,$$

where the sign of the resulting balance force is taken into account. With this simple modification, we can see what are the conditions for backstepping to occur, remarking that for the sigmoidal response of the pocket this condition holds for a broader spectrum of opposing forces. In Fig. 5 we show plots for the three cases discussed above.

As we can see, the concept of stalling can be splitted into two different ways of stopping the motor by applying an external force. In Ref. 6 backstepping in kinesin-1 is observed when loaded with very large and negative forces. Despite the reversibility of the motors such as the FO-F1-synthase, kinesin-1 does not hydrolyze ATP when walking

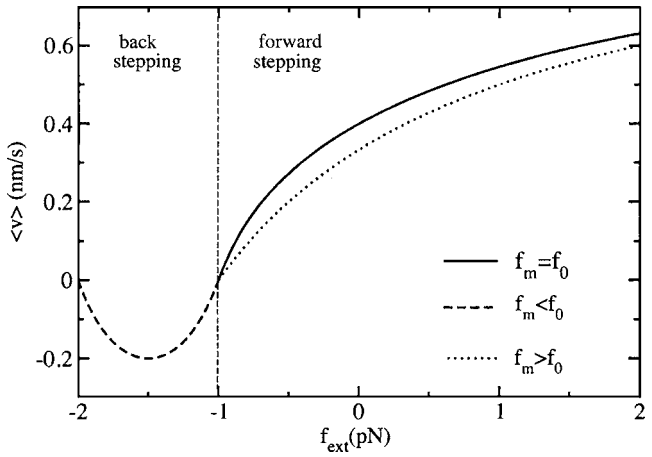

FIG. 5. Mean velocity vs the external force for a linear response of δx under a load. Now we have internal, mechanical, and chemical times. We set all the parameters fixed and equal to unity except f_m and f_0. The continuous line corresponds to a $f_m=f_0=1$ pN case. The dashed line corresponds to $f_m=1$, $f_0=2$ pN. The dotted line corresponds to $f_m=2$, $f_0=1$ pN. Note that all the continuous path holds also for dashed-line values. Both solid and dotted do not have values below -1 pN. Note the negative velocity section for the dashed line.

backward, but it keeps on consuming the energy from the nucleotide. In such a situation, the external mechanical force is greater than the motive force, but the cycle of ATP consumption is not stalled yet. This is the main reason to make such discrimination. We think that the mentioned experiment shows that in kinesin-1 the mechanical stall force is considerably lower than the force required to stop the ATP hydrolysis cycle, i.e., $-f_0$.

III. RESULTS

Our aim now is to use the experimental data of velocity versus substrate concentration and load of a particular motor to fit our formula and get the values of the free adjustable parameters. With this information we can guess which features are specific of a particular motor or which ones are common between two or all of them. It is expected that kinesin and RNAp will exhibit a considerable amount of similarities as both are mechanical enzymes powered by nucleotides.

A. A nonconservative force: The BFM

The BFM is a rotatory device that performs a torque on an helical flagella to propel the cell. It uses the electrochemical potential across the cytoplasmic membrane to perform the work. These engines work with a flux of protons in *Escherichia Coli* and Na^+ ions in alkalophiles and *marine Vibrio* species. Several experiments have been able to track their rotation by different techniques,[1,7] but only very recently[4] discrete steps have been observed. We will focus our attention toward Ref. 1 because they provide a wide and complete set of measurements that can be incorporated in our theoretical framework. In this experiment, a silica bead is attached to the flagellar filament. Then, rotating frequency of this bead is measured through a quadrant photodiode. The applied load is modulated through different sizes of the bead, thus the forcing is simply friction, and then the load is not conservative.

The substrate of this particular motor is the sodium Na^+ ion density gradient, which crosses the cytoplasmic membrane of the cell producing the rotation of the flagellar motor. Across the membrane, there is an electrochemical potential, which is the responsible for the sodium motive force, which we will write like τ_m.

We now proceed to calculate all the values for the different free parameters of the model. First, we need to know which is the step angle $\Delta\theta$ for each crossing ion, if there is a tight coupling between them. It is known [17] that BFM have different and independent torque generating units. The number of the units, depending on the particular device, can be from 5 to 9 in alkalophilic Bacillus, 5 to 8 in *V. alginolyticus*,[1] and at least 11 in *Escherichia coli*.[17] It is also known that about 1000 Na^+ ions[1] or 1200 protons[4] are required to perform a whole revolution of the motor. Focusing on sodium ions data, we can estimate the angle per ion,

$$\Delta\theta \sim \frac{2\pi}{1000} \sim 0.006 \text{ rad/Na}^+. \tag{15}$$

The chemical free energy due to the concentration difference between both sides of the membrane can be written as

$$\Delta G_{\text{chem}} = -k_B T \ln \frac{[\text{Na}^+]_{\text{ext}}}{[\text{Na}^+]_{\text{int}}}, \tag{16}$$

where $k_B T \simeq 4.1$ pN nm is the thermal energy, $[\text{Na}^+]_{\text{int}} = 30$ mM the ion concentration inside the membrane, and $[\text{Na}^+]_{\text{ext}}$ is the external concentration, which is modulated in the experiment. The concentration gradient between $[\text{Na}^+]_{\text{int}}$ and $[\text{Na}^+]_{\text{ext}}$ imposes an electrostatic gradient as well. The free energy for this effect is given by the membrane potential $\Delta\Psi$, which is about -150 mV. The total free energy is then

$$\Delta G = -k_B T \ln \frac{[\text{Na}^+]_{\text{ext}}}{[\text{Na}^+]_{\text{int}}} + \Delta\Psi. \tag{17}$$

We choose to use energy units in pN nm. We have then 1 mV=0.16 pN nm/e and $\Delta\Psi=-24$ pN nm/e. We substitute the previous values of the parameters to obtain

$$\Delta G = [-10.055 - 4.1 \ln[\text{Na}^+]_{\text{ext}}] \text{ pN nm}. \tag{18}$$

Now we can write the motive torque τ_m as

$$\tau_m = \frac{-\Delta G}{\Delta\theta}. \tag{19}$$

As the value we already have for $\Delta\theta$ is not precise yet, we can obtain another estimation and compare it to the previous one. From the experimental data we know that for different Na^+ concentrations, we have values for the torque which can be fitted from the experimental data in Ref. 1,

$$\tau_m \sim C_1 + C_2 \ln[\text{Na}^+]_{\text{ext}}, \tag{20}$$

where $C_1=1464$ pN nm and $C_2=586$ pN nm. We can see how these values correspond to different estimations of $\Delta\theta$. As the thermal energy is well known, C_2 is used to give $\Delta\theta=7\times10^{-3}$, in a good agreement with our previous estimation. On the other hand, the independent term can be used

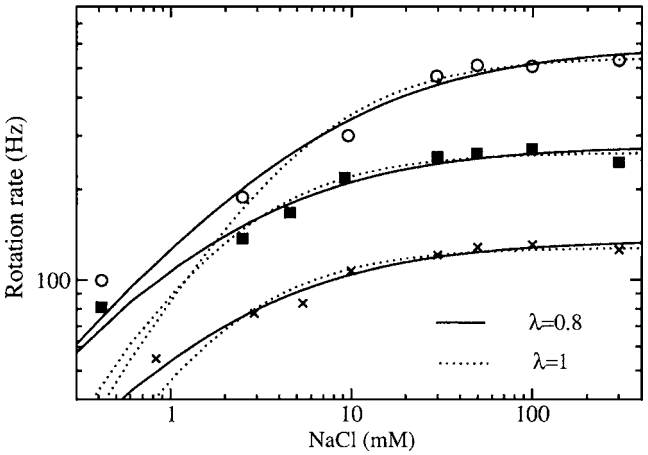

FIG. 6. Mean rotation rate vs $[Na^+]_{ext}$ concentration. Open circles, filled squares, and crosses correspond to beads of diameters of 0.60, 0.85, and 1.08 μM, respectively. The dotted lines are standard M-M fits. The solid lines correspond to a generalized interpretation of the law mass action, i.e., the rate of a reaction is proportional to $[S]^\lambda$, where if $\lambda=1$ we recover the classical version. For solid lines we use $\lambda=0.8$, which is in more agreement with the data at low substrate concentrations.

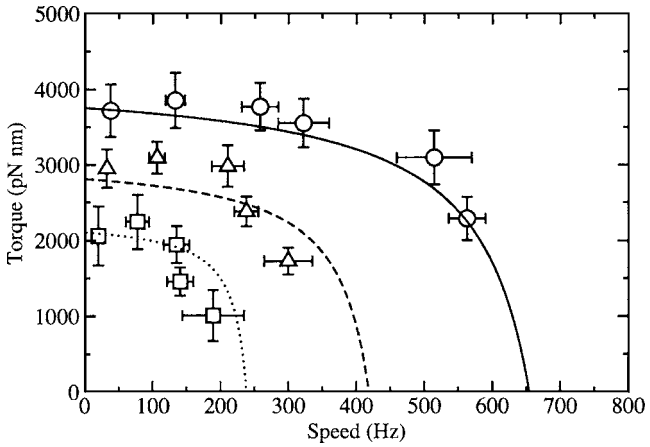

FIG. 7. Frequency vs the generated torque for the flagellar motor. Hereafter, points are always experimental data and lines are a fit from Eq. (20). Circles, triangles, and squares correspond to 50, 10, and 3 mM sodium concentrations, respectively. Notice how the stall torque is $[Na^+]_{ext}$ dependent.

to give a more precise value for the membrane potential, $\Delta\Psi=-151.2$ mV, which is in agreement with the value given in the Ref. 1.

We can now write down the frequency ν of the motor as a function of the external sodium concentration and of the external torque, which is nothing more than Eq. (13) divided by 2π,

$$\nu=\frac{\Delta\theta/2\pi}{a_0+\dfrac{a_1}{[Na^+]_{ext}^{\lambda}}+\dfrac{\gamma_r\Delta\theta^2}{10.245+4.1\ln[Na^+]_{ext}-\Delta\theta\tau_{ext}}}. \tag{21}$$

We recall that in the case of BFM motor we consider δx as a constant. There are some reasons to justify it. First, ions are considerably smaller than nucleotides, and they do not need a specific binding orientation, so a possible small decrease in the cross section of the cavity should not appreciably affect the rate on entrance. Secondly, in this motor the torque is transmitted through the torsion of the connecting axis which is far away from the cavities, which are not necessarily deformed then. But the main reason is that this nonconservative force is not active when the motor is not rotating, i.e., the bead does not perform a torque: it only resists it. Consequently we cannot exactly know whether a conservative force experiment would show that chemical times are appreciably affected by the load. On the one hand a_0 accounts for the sum of internal and for the adhesion time, put together since they do not depend on the load here. Then, $a_0=t_i+A/\delta x$. On the other hand a_1 modulates the influence of the effusive part of the chemical time and propose the expression $a_1=B/[S]^\lambda$. Here λ is the exponent of the law of mass action, which is not necessarily 1 as it seems to be the case of highly diffusive ions. In fact, we will use $\lambda=0.8$ which clearly fits better the frequency-concentration curves as seen in Fig. 6 for very low ion concentrations. In this motor we have not assumed that the chemical time depends on the external torque but only on the ion concentration. This is consistent with a picture where the ions do not have any difficulty to enter into the cavity.

In Fig. 7 we plot the frequency-torque curves for the fitted values of Table I. There are three cases which correspond to different ion concentrations. Note that in this case, it is found in the literature plots of the torque versus frequency. We only invert the expression to plot the data as it is presented in the original reference. The overall agreement is reasonably good considering the error that is introduced by the considerable technical difficulties of the experiment.

B. A conservative force: Kinesin-1 and RNAp

In this section we will simultaneously deal with two examples of molecular motors: the kinesin-1 and the RNAp, whose physical properties can be measured experimentally with optical trapping.[2,3] These motors have a certain amount of similarities and differences which our approach can discriminate extracting relevant information and interesting conclusions.

Both machines are linear motors walking along one-dimensional and polar tracks. They hydrolyze nucleotides in a well localized pocket, and most important for our purposes, both motors have chemical times that strongly depend on the load. As the external force is conservative we can also study the case of assisting loads, so we can obtain a wider response spectrum of the motor in the presence of a variety of forcing.

We start using the well known facts: kinesin performs 8 nm steps and stalls with forces of approximately ~5 pN,

TABLE I. Values of the parameters for the flagellar motor obtained by fitting Eq. (21) to the experimental data of Ref. 1.

Parameter	Value
$\Delta\theta$	7×10^{-3} rad
γ_r	0.1 pN nm s/rad
a_0	1.2×10^{-6} s
a_1	7.5×10^{-6} s mM$^\lambda$
λ	0.8 (dimensionless)

TABLE II. Values of the parameters for kinesin and RNAp motors, obtained by fitting experimental data from Refs. 2 and 3, respectively.

Parameter	Kinesin	RNAp
γ_t	~ 0 pN s/nm	~ 0 pN s/nm
t_i	0.003 s	0.034 s
A'	0.0178 s	0.016 s
B'	1.27 μM s	1.5 μM s
f_0	3.6+0.28 ln[ATP] pN	13.53 pN

while RNAp performs 0.37 nm steps and stalls with forces of $\sim$25 pN. While kinesin hydrolyzes ATP, RNAp can consume the four types of nucleotides ATP, GTP, CTP, and UTP, generally expressed as NTPs. In the experiment for RNAp, NTP concentrations are chosen in such a way that all the nucleotides bind the pocket with same rate. This set of relative concentrations is called $[\mathrm{NTP}]_{\mathrm{eq}}$.

First we will focus our attention to kinesin-1, using the experimental data of Refs. 2 and 5. The expression derived in Eq. (12) can be rewritten in a Michaelis–Menten form (identifying $[S]=[\mathrm{ATP}]$),

$$\langle v\rangle = \frac{v_{\max}[\mathrm{ATP}]}{k_M + [\mathrm{ATP}]}, \tag{22}$$

where

$$v_{\max} = \frac{L}{\frac{A}{\delta x} + t_i + \frac{\gamma_1 t}{f_m + f_{\mathrm{ext}}}} \tag{23}$$

and

$$k_M = \frac{B}{A + \delta x\left(t_i + \frac{\gamma_t L}{f_m + f_{\mathrm{ext}}}\right)}. \tag{24}$$

As both k_M and $u_{\max}$ are affected by the external load, we can interpret the effect as a mixed inhibition, as reported in Ref. 12. Now we proceed to fit this expression with the experimental data to get the free parameters. One first interesting result is that γ_t is very small, and consequently it implies that the mechanical characteristic time which is much lower than the other times. Thus setting $\gamma_t=0$, the equation for the velocity is

$$\langle v\rangle = \frac{L}{t_i + \frac{A'}{1+\tanh(C'(f_0+f_{\mathrm{ext}})-1)}} \times \frac{[\mathrm{ATP}]}{[\mathrm{ATP}] + \frac{B'}{A' + t_i \tanh(C'(f_0+f_{\mathrm{ext}})-1)}}, \tag{25}$$

where

$$A' \equiv \frac{2A}{l_x}, \quad B' \equiv \frac{2B}{l_x}, \quad C' \equiv \frac{2}{kl_x}, \tag{26}$$

and the sigmoidal response of δx has been used. We show in Table II the values that fit better the experimental data.

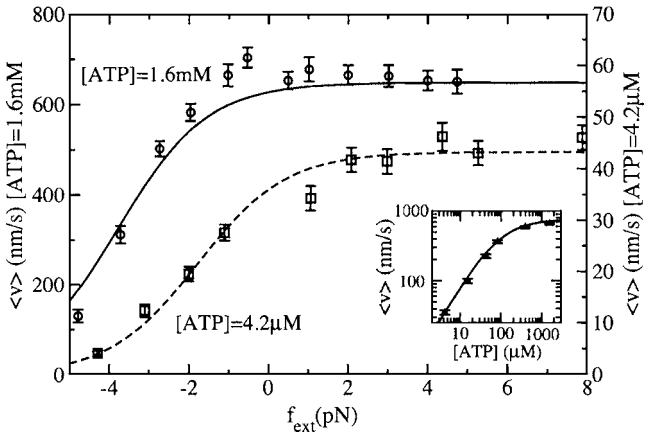

FIG. 8. Mean velocity vs the external force for the kinesin. Left vertical labels, solid lines, and open circles (○) correspond to [ATP]=1.6 mM, while right vertical labels, dashed lines, and open squares (□) correspond to [ATP]=4.2 μM. In the inset, we can see the mean velocity vs ATP concentration in the absence of external load. The lines correspond to the fit of Eq. (12) with paremeter values of Table II, and symbols from experimental data (Ref. 2).

It is important to remark that we have not found a constant value for f_0. Specifically, we have found that it depends on ATP concentration in a way that we have approximated as logarithmic. This can be interpreted as the effect of the entropic contribution in the total free energy,

$$\Delta G = \Delta G^0 + k_B T \ln \frac{[\mathrm{ATP}]}{[\mathrm{ADP}][P_i]}. \tag{27}$$

Some additional information can be extracted from the value of C'. If we consider that l_x is of the order of ATP size of $\sim$15 Å, then $k \sim 2/(1.5\times 0.45) \sim 3$ pN/nm, which gives an idea of how stiff is the pocket. In Fig. 8 we can see how our calculations and the experimental data fit together.

Now we perform a similar analysis to the RNAp motor. Again we obtain that we can neglect the mechanical time. Now $L=0.37$ nm and $[S]=[\mathrm{NTP}]$. In Table II we show the best fitted values of the free parameters which can be compared to the kinesin ones. In Fig. 9 we can compare our

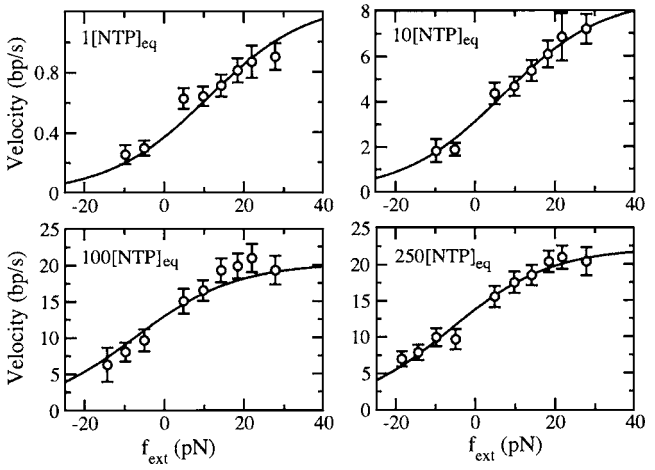

FIG. 9. Mean velocity, measured in bp/s, vs external force for RNAp. Left top, right top, left bottom, and right bottom correspond to [NTP]=1, 10, 100, and 250$[\mathrm{NTP}]_{\mathrm{eq}}$, respectively. The lines correspond to Eq. (12) with parameter values Table II, and symbols form experimental data of Ref. 3.

calculations by using Eq. (12) to the tabulated parameters versus the experimental results of Ref. 3 for four different NTP concentrations.

IV. DISCUSSION

In BFM, our theory reveals that there is no need for a load-dependent chemical time, as the sodium ions diffuse rapidly into the motor. Maybe extremely low ionic concentrations would require the introduction of such dependence, but it was not needed in the scale of the experiment of Ref. 1. It is stated in Ref. 18 that every model for BFM must include the soft linkage between the motor and the viscous load. This assumption is based on the compliance of the hook, which is measured in Ref. 19. However, we do not need to use such fact to justify the existence of the plateau region of the motor torque-speed curve. This plateau, which is nothing but a rapid decay of the velocity at high loads, can be explained by considering that the mechanical time slightly increases at low loads, while it diverges near the stall torque, and consequently it is not necessary to consider tow straight lines to fit the data as in Ref. 18. The concept of knee velocity point discussed in that reference can be understood as the torque value from which the mechanical time begins to dominate over the other processes, but it is not a kind of singular point in the curve.

Moreover, the coupling ratio in the BFM is probably 1, i.e., a single ion is tightly coupled with the rotation, but there is no conclusive evidence for such an assumption. In Ref. 4 they measure 0.24 rad steps, which correspond to 26 steps per revolution. This is precisely the periodicity of the FliG protein in the structure. However, the existence of a smaller periodicity in the steps is not discarded yet. It is estimated that around 1000 ions are needed to complete a revolution, so there is a possibility that an accumulation of several ions is needed to perform a step, but maybe this step can be decomposed in several substeps, each one corresponding to an ion transition. If the numbers above are confirmed, about 40 ions would be needed for a torque generating unit to complete its power stroke cycle.

For the BFM we can conclude that our approach is able to deal and fit the experimental data within a reasonable wide range of parameter values. The difficulties of the experiment make a finer approach unavoidable for now. No pocket assumption has been made, so the chemical time is not appreciably affected by the load.

In the case of NTP-driven motors, we can appreciate some differences and similarities between them. First, it is remarkable that the internal time for the RNAp, $t_i=0.034$ s, is an order of magnitude longer than for kinesin, $t_i=0.003$ s. This is consistent with a motor that, apart from transcriptional pauses, which are removed from the data, performs a more sophisticated task every cycle.[20] Concerning the substrate dependence of the stall force, our model suggests that in RNAp the stall force does not depend on the load, $f_0=13.53$ pN, while in kinesin it does, $f_0=3.6+0.28\ \ln[\mathrm{ATP}]$ pN. This dependence was observed in Ref. 5 even though more recent measurements[6] suggest that the stall force is [ATP] independent. However, we are trying to fit the data where the stall force does depend on [ATP], even if it is an artifact of the setup. In any case, this is an open question that more refined experiments should clarify. It is interesting to note that in the latter reference the external forces can be up to −15 pN, which clearly indicates that f_0 should have a stronger value.[21] However, the data provided in that reference lack more realizations to perform a detailed quantitative analysis of the mean velocity in the high-load regime. Additionally, we can see how C' is about ten times greater in the case of kinesin, $C'=0.45\ \mathrm{pN}^{-1}$, than in the case of RNAp, $C'=0.04\ \mathrm{pN}^{-1}$. Since both mechanoenzymes bind similar-size nucleotides, it is reasonable to suppose that l_x is similar as well in both motors. So then, as the stiffness is inversely proportional to the parameter C', the stiffness of the pocket in RNAp has to be considerably higher than in kinesin (of the order of ten times). This may be the reason why the value of f_0 for RNAp does not seem to depend on the substrate concentration. If the pocket is stiffer, it hardly changes its natural, load-free conformation. It is remarkable as well that A' and B' are very similar in both mechanoenzymes ($A'=0.0178$ s, $B'=1.27\ \mu$M s for kinesin-1, $A'=0.016$ s, $B'=1.5\ \mu$M s for RNAp) which reflects that binding times of the nucleotides do not appreciably differ between them. Mechanical time is negligible in kinesin and RNAp, which means that the power stroke mechanism occurs in a time scale which is much lower than other processes in agreement with the observed steplike trajectories. We expect other [NTP] motors as myosins and dyneins to have this feature as well, since the forces and the frictions involved in their motions imply physical velocities much greater than their corresponding chemical rates.

We thus conclude that the kinetics of kinesin and RNAp are regulated by very similar processes, even though some of them are quantitatively different. Nevertheless, experimental data from both devices can be understood under the same conceptual framework.

It is also worth to mention here that our approach does predict the existence of two different stalling forces: mechanical and chemical, which can stimulate some experiments to elucidate their real existence.

Summarizing, in this paper we have analyzed the kinetics of three different molecular motors with the intention of providing a general framework to deal with mechanochemical molecular engines. These three motors are a very representative set because all of them have been accurately measured in single molecule experiments. Our approach can enlighten the most relevant and specific properties of each one that should be taken into account in future more refined modelings.

ACKNOWLEDGMENTS

This work was supported by the Ministerio de Educación y Ciencia (Spain) under Project No. FIS2006-11452-C03-01 and Grant No. BES-2004-3208.

[1] S. Yoshiyuki, H. Hotta, M. Homma, and A. Ishijima, J. Mol. Biol. **327**, 1043 (2003).
[2] S. M. Block, C. L. Asbury, J. W. Shaevitz, and M. J. Lang, Proc. Natl. Acad. Sci. U.S.A. **100**, 2351 (2003).

[3] E. A. Abbondanzieril, W. J. Greenleaf, J. W. Shaevitz, R. Landick, and S. M. Block, Nature (London) **438**, 460 (2005).
[4] Y. Sowa, A. D. Rowe, M. C. Leake, T. Yakushi, M. Homma, A. Ishijima, and R. M. Berry, Nature (London) **437**, 916 (2005).
[5] K. Visscher, M. J. Schnitzer, and S. M. Block, Nature (London) **400**, 184 (1999).
[6] N. J. Carter and R. A. Cross, Nature (London) **435**, 308 (2005).
[7] H. C. Berg and L. Turner, Biophys. J. **65**, 2201 (1993).
[8] D. Keller and C. Bustamante, Biophys. J. **78**, 541 (2000).
[9] M. E. Fisher and A. B. Kolomeisky, Proc. Natl. Acad. Sci. U.S.A. **98**, 7748 (2001).
[10] F. Jülicher, A. Ajdari, and J. Prost, Rev. Mod. Phys. **69**, 1269 (1997).
[11] K. I. Skau, R. B. Hoyle, and M. S. Turnery, Biophys. J. **91**, 2475 (2006).
[12] A. Ciudad and J. M. Sancho, Biochem. J. **390**, 345 (2005).
[13] J. V. Grigoriev, Y. A. Makhnovskii, A. M. Berezhkovskiia, and V. Y. Zitserman, J. Chem. Phys. **116**, 9574 (2002).
[14] T. Sakamoto, A. Yildiz, P. R. Selvin, and J. R. Sellers, Biochemistry **44**, 16203 (2005).
[15] C. L. Asbury, A. N. Fehr, and S. M. Block, Science **302**, 2130 (2003).
[16] N. Naber, T. J. Minehardt, S. Rice, X. Chen, J. Grammer, M. Matuska, R. D. Vale, P. A. Kollman, R. Car, R. G. Yount, R. Cooke, and E. Pate, Science **300**, 798 (2003).
[17] S. W. Reid, M. C. Leake, J. H. Chandler, C. Lo, J. P. Armitage, and R. M. Berry, Proc. Natl. Acad. Sci. U.S.A. **103**, 8066 (2006).
[18] J. Xing, F. Bai, R. Berry, and G. Oster, Proc. Natl. Acad. Sci. U.S.A. **103**, 1260 (2006).
[19] S. M. Block, D. F. Blair, and H. C. Berg, Nature (London) **338**, 514 (1989).
[20] H. Y. Wang, T. Elston, A. Mogilner, and G. Oster, Biophys. J. **74**, 1186 (1998).
[21] M. Dixon and E. C. Webb, *Enzyme Inhibition and Activation in Enzymes*, 3rd ed., edited by M. Dixon, E. C. Webb, C. J. R. Thorne, and K. F. Tipton (Longman, London, 1979), pp. 332–467.